The Astrophysical Journal, 578:657–663, 2002 October 10

OPACITY DATA FOR HCN AND HNC FROM A NEW AB INITIO LINE LIST

Gregory J. Harris, Oleg L. Polyansky,[1] and Jonathan Tennyson[2]
Department of Physics and Astronomy, University College, London WC1E 6BT, UK
Received 2002 May 7; accepted 2002 June 13

ABSTRACT

A new extensive ab initio rotation-vibration HCN/HNC line list is presented. The line list contains rotation-vibration energy levels, line frequencies, and line strengths for transitions between states with energy less than 18,000 cm^{-1} and with $J \leq 60$. This line list greatly improves the quality and range of HCN/HNC data available. It is presently the most extensive and most accurate ab initio HCN/HNC line list in existence. It is hoped that this data set will be used in models of C star atmospheres and elsewhere.

Subject headings: line: identification — molecular data

1. INTRODUCTION

HCN and HNC are important molecules throughout astronomy; for example, HCN has been observed in comets (Huebner, Snyder, & Buhl 1974; Irvine et al. 1996), planetary atmospheres (Hidayat et al. 1997), molecular clouds (Hatchell, Millar, & Rodgers 1998; Hirota et al. 1998), carbon star atmospheres (Aoki, Tsuji, & Ohnaka 1998, 1999; Bieging, Shaked, & Gensheimer 2000), and circumstellar masers (Bieging 2001). In fact, prior to its detection in the interstellar medium in 1971 by the radio astronomers Snyder & Buhl (1971, 1972), HNC had been observed in the laboratory only by means of matrix isolation spectroscopy.

Of particular interest to us is the role of HCN in C star atmospheres. Calculations by Eriksson et al. (1984) and Jørgensen et al. (1985) suggest that the proper detailed treatment of the vibration-rotation spectrum of HCN can have profound effect on the structure of the C star model atmospheres. Jørgensen et al. (1985) found that including HCN opacity in their model atmospheres caused the atmosphere to expand by a factor of 5 and lowered the gas pressure of the surface layers by 1 or 2 orders of magnitude.

Several sets of HCN opacity data have been used in model C star atmospheres. These include the ab initio opacity data of Jørgensen et al. (1985), the empirical data of Jørgensen (1990), and the recent line list of Aoki et al. (1998). The ab initio opacity data of Jørgensen et al. (1985) have been recently used by Loidl et al. (1999) in their model C star atmospheres. They contain band frequencies and intensities for transitions between states with energy less than 10,000 cm^{-1}. The data of Jørgensen (1990) use the experimental data of Smith et al. (1987, 1989) with empirical estimates of the intensities of the hot bands. These data include high-frequency bands such as the (40^00) C-H stretch overtone. Finally, the data of Aoki et al. (1998) are based on experimental data that have become available since the work of Jørgensen (1990). They cover a limited number of bands, the (01^10), (02^00), (100), (01^11), and (100)–(01^10) transitions and their hot bands up to $v_2 = 4$.

All data sets cover the most intense HCN transitions, which are primarily the C-H stretch and bend fundamentals and some of their hot bands. The effects of these two modes at 3 and 14 μm are well known. However, all these data sets have their weaknesses. The data of Jørgensen (1990) are relatively inaccurate for the hot bands and cover a limited number of bands. The data of Aoki et al. (1998) also cover only a limited number of bands and their hot bands up to $v_2 = 4$. The ab initio data of Jørgensen et al. (1985) cover all transitions involving states less than 10,000 cm^{-1} above the zero point energy but are inaccurate by today's standards. Furthermore, HCN is believed to be an important opacity source in C stars up to $T_{\rm eff} \sim 2800$ K (Eriksson et al. 1984). At these high temperatures, states with energy greater than 10,000 cm^{-1} may contribute significantly to the overall opacity. Finally, HNC has been neglected by all workers to date. In thermodynamic equilibrium, the HNC/HCN ratio for $T = 2000$–4000 K is between 0.05 and 0.34 (Barber, Harris, & Tennyson 2002). The transition dipoles of HNC are considerably stronger than comparable transitions of HCN, which increases the likelihood that HNC will have a significant effect on opacity.

To increase the amount of HCN and HNC data available and to fill in the gaps in the existing data, we have calculated a new extensive HCN/HNC line list. This line list contains rotation-vibration energy levels, line frequencies, and line strengths for transitions involving states with energy less than 18,000 cm^{-1} and with values of the rotational quantum number, J, of $J \leq 60$.

In § 2, the calculation of the line list is discussed, and in § 3 the results of the calculation are presented. Finally, in § 5 we discuss the results and conclude.

2. CALCULATION

Querci & Querci (1970) claimed to detect the (40^00) HCN stretching overtone at 791 nm in the atmosphere of the C star UU Aur. Later, Giguere (1973) tentatively identified the (30^00) HCN stretching overtone at 1 μm in the same star. However, using a new line list based on experimental data, Jørgensen (1990) disputed that any bands beyond 1.5 μm could be observed in C star atmospheres. Therefore, the aim of this work is to compute the HCN and HNC transitions, including hot bands contributing significantly, longward of 1.5 μm. To give an accurate value for the band intensity and the distribution of the intensity across the band, the data must extend to a high value of J, such that for a given band, transitions to and from the highest value of J have only a fraction of the peak line intensity of band. As a result, we

[1] Permanent address: Institute of Applied Physics, Russian Academy of Science, Uljanov Street 46, Nizhnii Novgorod, Russia 603024.
[2] Corresponding author; j.tennyson@ucl.ac.uk.

have extended our line list to $J \leq 60$. At $T = 3000$ K with energy levels less than 18,000 cm^{-1} and $J \leq 60$, the rotational-vibrational partition function is calculated to be 35,653. This is 93% of the rotationally converged value of 38,405, reported in a forthcoming paper (Barber et al. 2002). This gives an indication that the line list reported here accounts for approximately 93% of the opacity of HCN/HNC at $T = 3000$ K.

The accuracy of the nuclear motion calculation depends on the accuracy of the potential energy surface (PES) and dipole moment surface (DMS) used in the calculation. Therefore, it is desirable to use the most accurate PES and DMS available. There are currently three ab initio semiglobal HCN/HNC PES available: the ANO/CCSD(T) PES of Bowman et al. (1993), the PES of Varandas & Rodrigues (1997), and the VQZANO+ PES covered in our earlier paper (van Mourik et al. 2001). Of these surfaces, the VQZANO+ surface uses the largest electronic basis set. As a result, in general, the band origins and intensities calculated with the VQZANO+ surface reproduce more closely the laboratory data than do those calculated with either of the other two semiglobal PES (see van Mourik et al. 2001). This surface is also capable of reproducing quite subtle effects observed in laboratory experiments; see Harris, Polyansky, & Tennyson (2002). Thus, for the calculations performed here we use the VQZANO+ PES.

The ab initio VQZANO+ PES simultaneously fits 1527 ANO/CCSD(T) points calculated by Bowman et al. (1993) with 242 points calculated at the higher cc-pCVQZ/CCSD(T) level. The surface is morphed with 17 aug-cc-pCVQZ/CCSD(T) points calculated in the HNC region of the PES, to improve the representation of the HNC part of the surface. To improve the rotational representation, the VQZANO+ surface is also adjusted to coincide with three cc-pCV5Z/CCSD(T) points calculated at the critical points of the HCN/HNC system. The VQZANO+ PES includes relativistic and adiabatic corrections, which are often neglected when constructing an ab initio PES.

There are three semiglobal dipole moment surfaces (DMSs) available; these are the TZP/AQCC DMS of Jakubetz & Lan (1997), the aug-cc-pCVTZ/CCSD(T) DMS of Bowman et al. (2001), and the cc-pCVQZ/CCSD(T) DMS of van Mourik et al. (2001). The DMS of Jakubetz & Lan (1997) was calculated with the smallest basis of these three DMSs; the intensities calculated with it compare with laboratory data far less favorably than do calculations with the DMS of van Mourik et al. (2001; see Harris et al. 2002). The DMS of Bowman et al. (2001) uses fewer points and a smaller basis than the van Mourik et al. (2001) DMS. The van Mourik et al. (2001) DMS, as a result, is the best available DMS and the one that is employed here.

To allow the calculation of HCN and HNC energy levels simultaneously, the calculation was performed in Jacobi coordinates. The coordinate r was chosen to represent the C-N distance, and the R coordinate was chosen to be the H to C-N center of mass distance. Finally, the angular coordinate γ is the angle between the R and r coordinates; the HCN minimum is located at $\gamma = 0$, and the HNC minimum is at $\gamma = \pi$.

Our vibrational, rotational, and transition dipole calculations were performed with the DVR3D program suite (Tennyson, Henderson, & Fulton 1995), which uses an exact kinetic energy (EKE) operator and a discrete variable representation (DVR) for the vibrational motions. Jacobi coordinates were used with Legendre polynomials to give the angular grid points and Morse oscillator-like functions for the radial grids. Thirty-five grid points were used for the R coordinate, 21 for the r coordinate, and 50 for the angular coordinate. This basis was optimized to obtain a balance between the level of convergence and the available computer resources. This basis is large enough to converge all calculations reported here and is the same as used in our previous calculation (Harris et al. 2002). The parameters for the Morse oscillator-like basis in the r coordinate are $r_e = 2.3a_0$, $D_e(r) = 29.0E_h$, and $\omega_e(r) = 0.0105E_h$. The parameters for the Morse oscillator-like basis in the R coordinate are $R_e = 3.2a_0$, $D_e(R) = 5.0E_h$, and $\omega_e(R) = 0.004E_h$. Where r_e is the equilibrium distance, D_e is the dissociation energy and ω_e is the harmonic frequency (see Tennyson et al. 1995).

The huge number of lines that were calculated required a large amount of processing power. This made it necessary to parallelize the processor-intensive routines of the DVR3D codes. The openMP FORTRAN API multiprocessing directives (openMP Consortium 2002)[3] with the MIPSpro 7 FORTRAN 90 compiler (MIPSpro, Silicon Graphics Inc. 2002)[4] on the "Miracle" 24 processor SGI Origin 2000 computer were used to perform the parallelization. The most processor-intensive module of the DVR3D suite is DIPOLE3, which calculates dipole transition strengths between states that are not rigorously dipole forbidden. One loop of this module calls a rank 1 matrix update subroutine and consumes 95% of the run time. By parallelizing this loop, we were able to reduce the run time by up to a factor of about 5 when running on eight processors, depending on computer load.

3. RESULTS

The line list contains all HCN/HNC transitions involving rotational-vibrational energy levels below 18,000 cm^{-1} and with $J \leq 60$. There are just under 400 million lines and over 168,000 energy levels in the full data set. This is a vast amount of data that requires a lot of storage space. To fully describe each of the 400 million records requires approximately 20 Gbytes. This size of file is not easily manipulated or ported from machine to machine. Ideally, we would like to reduce the overall size of the file and split it into smaller blocks of data that cover specific frequency ranges. The following discussion covers the compact format that has been chosen to store the data.

Each rotational-vibrational state is often described by a set of quantum numbers, some of which are good quantum numbers and some of which are approximate quantum numbers. The good quantum numbers are the rotational quantum number J, the rotational parity, and n, the state number within the J-parity symmetry block. The approximate quantum numbers are the vibrational quantum numbers v_1, v_2, and v_3, and the vibrational angular momentum l. The good quantum numbers are output from the calculation in conjunction with the energy levels and the wave functions, whereas the approximate quantum numbers are assigned after the calculation.

[3] See http://www.openmp.org.

[4] See http://www.sgi.com/developers/devtools/languages/mipspro.html.

The six integers required to describe the transition are the good quantum numbers of the upper and lower states. The four floating point variables required to describe the transition are the energies of the upper and lower states (E', E''), the transition frequency (ν), and the Einstein A-coefficient (A_{ij}). There are two facts that allow us to store the data in a more compact format. These are:

1. ν can be calculated from E' and E''.
2. The energy and quantum numbers of each rotational-vibrational state are repeated throughout the data file.

Consequently, the full transition file can be split into an energy level file and a transition file. The good quantum numbers and energies of each level are stored in the energy level file. Where approximate quantum numbers have been assigned, they are also given. An integer flag that identifies the state as HCN, HNC, a delocalized state, or unassigned is also given. Finally, each level is given a unique index integer. The index numbers of the upper and lower state and the line strength are stored in the transition file. This is a more efficient way of storing the line list, resulting in nearly a factor of 3 reduction in file size. Short extracts from the energy level file and the transition file are given in Tables 1 and 2.

It is often the case that only a small portion of the spectrum is of interest. It was therefore decided that the file be split into smaller files, each with a specific frequency range, thereby allowing only the spectral regions of interest to be downloaded. Further to this, the data also have been sorted into frequency order. For the Einstein A-coefficient, the data beyond the sixth significant figure are meaningless; consequently, data are given only to the sixth significant figure. For reasons of compatibility, the data have been converted to text format and gzipped.

The Einstein A_{ij}-coefficient, in s^{-1}, is related to the integrated line absorption intensity, I_i, in units of cm^{-2} atm^{-1}, by

$$I_i = \frac{3.507293 \times 10^{-6} \times (2J' + 1)}{Q_{\rm vr}\nu^2} \left(\frac{273.15}{T}\right) \exp\left(\frac{-E''}{kT}\right) \times \left[1 - \exp\left(\frac{-hc\nu}{kT}\right)\right] A_{if} \ , \quad (1)$$

where ν is the wavenumber in cm^{-1} of the line, h is Planck's constant, c is the speed of light, k is Boltzmann's constant, E'' is the energy of the lower rotational-vibrational energy level, T is the temperature, and $Q_{\rm vr}$ is the rotational-vibrational partition function.[5]

TABLE 1

Extract from the Full Energy Level File

Index	J	p[a]	n	E[b] (cm^{-1})	i[c]	v_1	v_2	l	v_3
1.....	0	1	1	0.000000	0	0	0	0	0
2.....	0	1	2	1414.915929	0	0	2	0	0
3.....	0	1	3	2100.582377	0	0	0	0	1
4.....	0	1	4	2801.459102	0	0	4	0	0
5.....	0	1	5	3307.745835	0	1	0	0	0
6.....	0	1	6	3510.991764	0	0	2	0	1

[a] If $p = 1$, this is an e state; if $p = 0$, this is an f state.

[b] This is the energy of the level relative to the HCN ground state. The zero-point energy is 3481.5053 cm^{-1}.

[c] This flag denotes the structure of the molecule in this state. Here $i = 0$ denotes HCN, $i = 1$ denotes HNC, $i = 2$ denotes a delocalized state, and $i = 3$ denotes an unassigned state.

TABLE 2

Extract from the Transition File

Index i	Index j	A_{ij}[a] (s^{-1})
6530	9178	0.328590D−21
157848	158599	0.354054D−15
19118	15561	0.151754D−16
40575	44648	0.918852D−18
32589	30544	0.113946D−13

[a] This is the Einstein A-coefficient of the transition between state i (upper) and state j (lower). The A-coefficient is presented in *FORTRAN* syntax, in which "D" denotes an exponent in a fashion identical to "E."

To generate some simple absorption spectra, one needs to obtain k_ν, the absorption coefficient or opacity function at frequency or wavenumber ν. The absorption coefficient of the spectrum is given by

$$k_\nu = \sum_i I_i f_i(\nu - \nu_{0,i}) \ , \quad (2)$$

where $f_i(\nu - \nu_{0,i})$ is the line profile and $\nu_{0,i}$ is the line center of line i. Once k_ν has been obtained, the Lambert-Beer law can be used to generate spectra. The Lambert-Beer law gives the intensity of a beam of radiation passing through a gas of pure HCN, with path length l and pressure p:

$$I_\nu = I_\nu(0) \exp(-k_\nu p l) \ , \quad (3)$$

where $I_\nu(0)$ is the initial intensity of the beam and k_ν is the absorption coefficient or opacity function. The integrated absorption, I_i, of line i is found from the absorption coefficient of the line, $k_{\nu,i}$, by

$$I_i = \int_{-\infty}^{+\infty} k_{\nu,i} \, d\nu \ . \quad (4)$$

The integrated absorption for the complete spectrum is thus

$$I = \sum_i I_i \ . \quad (5)$$

Here I is of limited use. Clearly, to calculate k_ν, one would need to know the line profile of each line and be able to sum over all lines. However, equations (2) and (4) suggest that k_ν for the spectrum in the interval ν to $\nu + \Delta\nu$ can be found more simply. This we do by summing I_i for all lines in the frequency interval $\nu - \nu + \Delta\nu$ and dividing by $\Delta\nu$. This frequency binning method gives an approximate average value for k_ν in the region ν to $\nu + \Delta\nu$. It also has the effect of reducing the resolution of the full spectrum to $\nu/\Delta\nu$. Frequency-binned opacity data have been presented by, for example, Schryber, Miller, & Tennyson (1995) and Neale, Miller, & Tennyson (1996). This method is adequate to illustrate the usefulness of the line list and obtain some simple

[5] Both the energy level file and the frequency-ordered transition files can be retrieved by (1) anonymous ftp to ftp://ftp.tampa.phys.ucl.ac.uk; change to the directory/pub/astrodata/HCN, or (2) via the TAMPA group Web page http://www.tampa.phys.ucl.ac.uk; follow the links for "Astrodata and Molecular Data," then "Astrodata," then "HCN." A decompaction code is provided, which is described in the accompanying "readme" file.

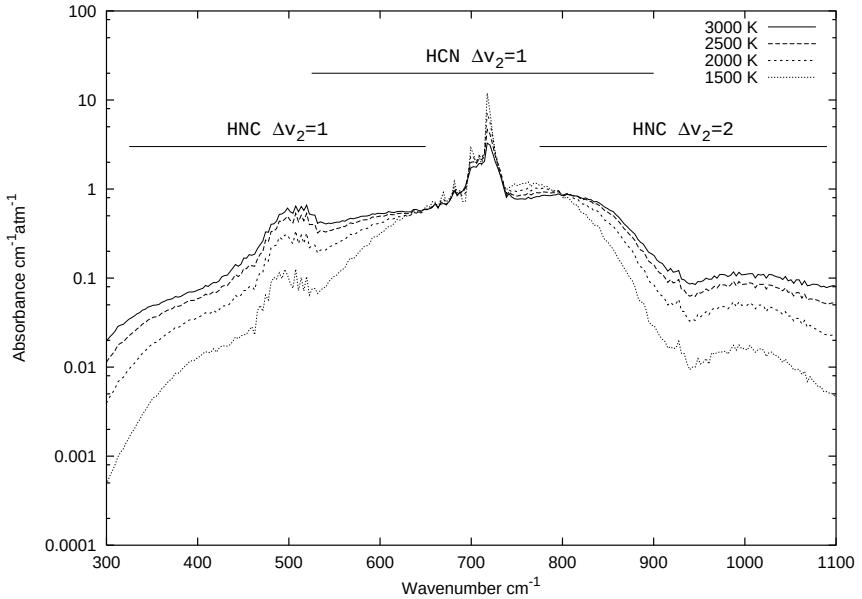

FIG. 1.—Absorption coefficient at $T = 1500$, 2000, 2500, and 3000 K at STP, in the region of the HCN and HNC bend fundamentals

absorption spectra. There are more sophisticated methods for opacity sampling that are beyond the scope of this work.

4. DISCUSSION

To demonstrate the usefulness of our line list, we now compare our opacity data with observed stellar spectra. The resolving power of the *Infrared Space Observatory* (*ISO*) short-wavelength spectrometer (SWS) in its low-resolution mode (SWS01) is about 200 (*ISO* Data Centre 2002).[6] This is the resolution at which Aoki et al. (1998) have observed C star spectra. So for spectra of comparable resolution, integrated absorption intensities have been put into bins of 3 cm^{-1}. Figures 1 and 2 show the resulting absorption coefficient (k_ν) in the spectral region of 300–1100 and 1100–3900 cm^{-1} at temperatures of 1500, 2000, 2500, and 3000 K. In the 300–1100 cm^{-1} interval, there are over 73 million lines; the main features are a result of $\Delta v_2 = 1$ HCN and HNC bending fundamentals and hot bands, centered on 715 and 465 cm^{-1}, respectively. In the 1100–3900 cm^{-1} frequency interval, there are over 165 million lines and several strong absorption features. These are the HCN $\Delta v_2 = 2$ overtone and its hot bands at ~1400 cm^{-1}, the HNC CN stretch fundamental and hot bands at ~2000 cm^{-1}, the HCN (10^00)–(01^10) band and its hot bands at ~2600 cm^{-1}, the HCN HC stretch fundamental and hot bands at ~3300 cm^{-1}, and the HNC HN stretch fundamental and hot bands at ~3660

[6] See http://isowww.estec.esa.nl.

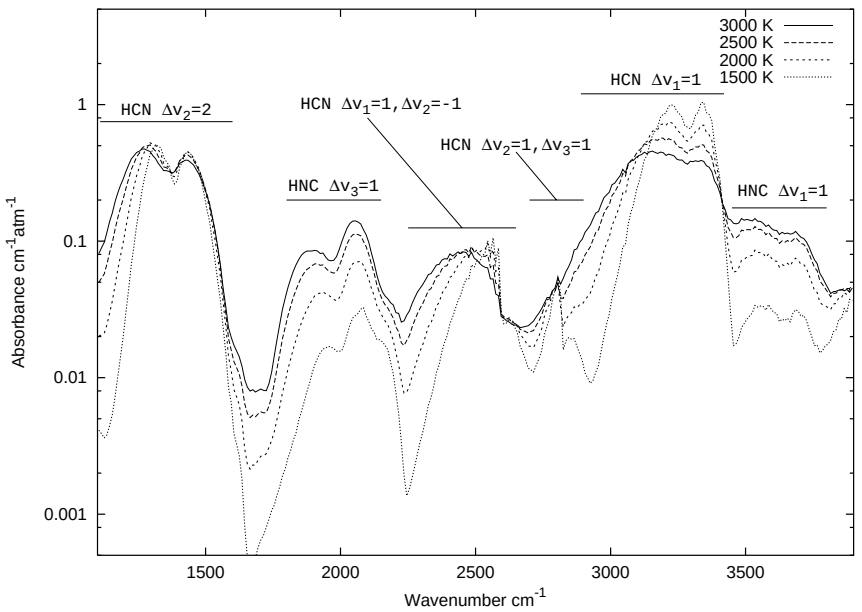

FIG. 2.—Absorption coefficient at $T = 1500$, 2000, 2500, and 3000 K at STP, in the region of the HCN and HNC stretch fundamentals

cm^{-1}. The HCN CN fundamental, its hot bands, the $\Delta v_2 = 3$ overtone, and hot bands at $\sim$2100 cm^{-1} are just discernible, as is the Q-branch of the (01^11)–(000) band at $\sim$2800 cm^{-1}. In both spectral ranges, HNC features contribute significantly to the opacity and lie in regions where there is little HCN absorption. We have used HCN/HNC partition functions of 3523.9, 8731, 19,288, and 38,405 at $T = 1500$, 2000, 2500, and 3000 K, respectively. These are rotationally converged values and will be reported in a forthcoming paper (Barber et al. 2002).

The effect of temperature on opacity is evident in Figures 1 and 2. In general, with increasing temperature, the absorption features resulting from strong HCN bands broaden, while their peak absorption decreases. This is a result of the excited HCN states becoming more populated, while the population of the HCN ground state decreases. Consequently and not surprisingly, the hot bands become responsible for more absorption as temperature increases. For HNC, as temperature increases, the strong HNC features broaden and their peak absorption increases. This is primarily a result of the population of HNC increasing with respect to HCN as temperature increases. The ratio of the intensity of the HCN HC stretch fundamental to the HNC HN stretch fundamental may prove to be a useful tool for obtaining temperature estimates. The temperature dependence of the HNC/HCN ratio will be discussed in detail in Barber et al. (2002).

To generate some simple absorption spectra, we use the Lambert-Beer law (eq. [3]). This allows a determination of the transmittance $[I/I(0)]$ of the beam, from κ_ν. Figure 3 shows the spectrum generated with our HCN/HNC opacity function, over the wavelength range 2.6–8 μm. This range is comparable to the range over which Aoki et al. (1998) measured the spectra of six C stars. Most of the main features in the HCN/HNC spectra (Fig. 3) appear to correlate well with the stellar spectra. For example, the 3.2, 4, and 7–8 μm features are present in both HCN/HNC and the stellar spectra of Aoki et al. (1998). The $\sim$5 μm HNC CN stretch features present in the HCN/HNC spectrum may be present in the stellar spectra. However, this is difficult to confirm; in the case of the HNC CN stretch feature, there is absorption from other molecular species, possibly C_3 (Aoki et al. 1998).

Aoki et al. (1998) have also taken higher resolution spectra of TX-Psc and WZ Cas in the 2.75–4.2 μm region. They used *ISO*'s SWS06 spectrometer, which has a resolution of around 1500. For comparison with these stellar spectra, we have calculated an HCN/HNC spectrum in the same region (see Fig. 4). To aid the reader, we have also plotted the spectrum of WZ Cas taken by Aoki et al. (1998) in Figure 4; the stellar spectrum has not been normalized. The two major features, at 3.2 and 4 μm of the spectrum of WZ Cas, are present in the HCN/HNC spectra. The 4 μm feature is attributable to the (10^00)–(01^10) band and its hot bands. The $\sim$2.8 μm HNC HN stretch feature present in the HCN/HNC spectrum may also be present in the stellar spectrum. A more detailed comparison, which could include a proper temperature determination, must await a full stellar model based on our new data.

The C star synthetic spectra calculated by Aoki et al. (1998) indicate that the predicted strength of the 4 μm absorption feature is particularly sensitive to the amount of hot band data used. The HCN opacity data used by Aoki et al. (1998) are based upon experimental data; they include transitions with bend excitations up to $v_2 = 4$. The limited nature of these data resulted in a considerable discrepancy between the synthetic and observed spectra of Aoki et al. (1998). In an attempt to better model this feature, Aoki et al. (1998) used an empirical extension to their data to extend it up to hot bands containing $v_2 = 9$. The synthetic spectra calculated with the extended HCN data compare considerably better with the observed spectra. The data used by Aoki et al. (1998) are considerably less extensive than the data presented here. Our data will not suffer from this lack of hot band data. Aoki et al. (1998) identified the Q-branch of the (01^11)–(00^00) overtone in the spectrum of WZ Cas.

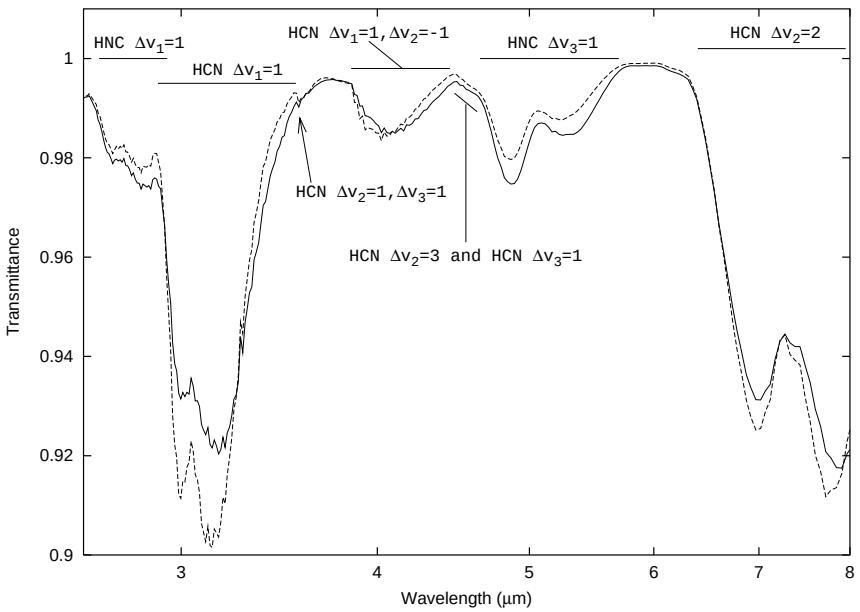

FIG. 3.—Transmittance (I/I_0) using a path length of 2 cm at 1 atm at $T = 3000$ K (*solid line*) and $T = 2500$ K (*dashed line*). The size of the bins is $\sim$0.01 μm.

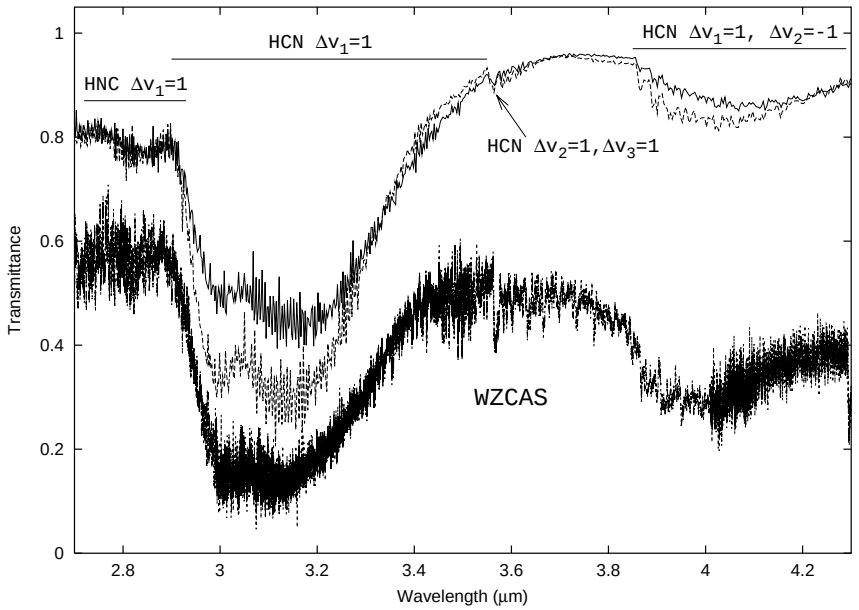

FIG. 4.—Transmittance (I/I_0) using a path length of 20 cm at 1 atm at $T = 3000$ K (*solid line*) and $T = 2500$ K (*dashed line*). The wavenumber range selected is in the region of the HCN and HNC stretching fundamentals and the $\Delta v_2 = 2$ overtone. The size of the bins is $\sim$0.002 μm. The lower spectrum is the unnormalized spectrum of the C star WZ Cas taken by Aoki et al. (1998). The stellar spectrum is on an arbitrary linear scale with a constant subtracted to stagger the spectra.

The Q-branch of this band is visible in the HCN/HNC spectrum at $\sim$3.55 μm but is much less pronounced than in the model atmosphere spectra of Aoki et al. (1998). The $\sim$2.85 μm HNC HN stretch feature present in the HCN/HNC spectrum is perhaps visible in the spectrum of WZ Cas. This is another and possibly the most promising region in which HNC could be looked for in C stars. If detected, the ratio of the peak intensity of the HNC $\Delta v_1 = 1$ bands to the HCN $\Delta v_1 = 1$ bands may prove a useful tool with which to estimate temperature.

5. CONCLUSION

The main HCN features in the ab initio HCN/HNC spectra presented here are in good qualitative agreement with the HCN features in the C star spectra observed by Aoki et al. (1998). This shows the usefulness of this new HCN/HNC line list. The data presented here indicate that if HCN and HNC are in thermodynamic equilibrium, HNC will play a significant role in the opacity of HCN containing C stars. Possible regions in which HNC might be detected in C stars have been identified as the regions of the HNC fundamentals at $\sim$2.8, $\sim$5, and $\sim$20 μm. The $\sim$2.8 μm feature looks like the most promising region in which to observe HNC. If observed, the ratio of the peak intensity of the HNC $\Delta v_1 = 1$ ($\sim$2.8 μm) absorption feature to the HCN $\Delta v_1 = 1$ ($\sim$3.1 μm) absorption feature may be a useful tool for obtaining temperature estimates.

In conclusion, the line list presented here is the most extensive HCN/HNC data set in existence. The line list is more accurate and more extensive than the ab initio HCN opacity data of Jørgensen et al. (1985), which is used in the recent model C star atmospheres of Loidl et al. (1999). It is considerably more extensive than the data of Aoki et al. (1998), which are based upon experimental data. Therefore, the use of the line list in a full stellar model should result in important effects. This line list is publicly available for use in stellar atmosphere models and otherwise.

We thank Callum Wright for the great deal of help he provided with computer system issues. We thank Hugh Jones for extracting the spectrum of WZ Cas from the *ISO* public archives. We thank the UK Particle Physics and Astronomy Research Council (PPARC) for Ph.D. studentship funding. The calculations reported in this work were carried out on the Miracle 24-processor Origin 2000 supercomputer at the HiPerSPACE computing center, UCL, which is partly funded by PPARC.

REFERENCES

Aoki, W., Tsuji, T., & Ohnaka, K. 1998, A&A, 340, 222
———. 1999, A&A, 350, 945
Barber, R. J., Harris, G. J., & Tennyson, J. J. 2002, J. Chem. Phys., submitted
Bieging, J. H. 2001, ApJ, 549, L125
Bieging, J. H., Shaked, S., & Gensheimer, P. D. 2000, ApJ, 543, 897
Bowman, J. M., Gazdy, B., Bentley, J. A., Lee, T. J., & Dateo, C. E. 1993, J. Chem. Phys., 99, 308
Bowman, J. M., Irle, S., Morokuma, K., & Wodtke, A. 2001, J. Chem. Phys., 114, 7923
Eriksson, K., Gustafsson, B., Jørgensen, U. G., & Nordlund, Å. 1984, A&A, 132, 37
Giguere, P. T. 1973, ApJ, 186, 585
Harris, G. J., Polyansky O. L., & Tennyson, J. 2002, Spectrochim. Acta, 58, 673
Hatchell, J., Millar, T. J., & Rodgers, S. D. 1998, A&A, 332, 695
Hidayat, T., Marten, A., Beźard, B., Gautier, D., Owen, T., Matthews, H. E., & Paubert, G. 1997, Icarus, 126, 170
Hirota, T., Yamamoto, S., Mikami, H., & Ohishi, M. 1998, ApJ, 503, 717
Huebner, W. F., Snyder, L. E., & Buhl, D. 1974, Icarus, 23, 580
Irvine, W. M., et al. 1996, Nature, 383, 418
Jakubetz, W., & Leong Lan, B. 1997, Chem. Phys., 217, 375
Jørgensen, U. G. 1990, A&A, 232, 420
Jørgensen, U. G., Almlöf, J., Gustafsson, B., Larsson, M., & Siegbahn, P. 1985, J. Chem. Phys., 83, 3034
Loidl, R., Höfner, S., Jørgensen, U. G., & Aringer, B. 1999, A&A, 342, 531

Neale, L., Miller, S., & Tennyson, J. 1996, ApJ, 464, 516
Querci, M., & Querci, F. 1970, A&A, 9, 1
Schryber, J. H., Miller, S., & Tennyson, J. 1995, J. Quant. Spectrosc. Radiat. Transfer, 53, 373
Smith, A. M., Coy, S. L., Klemperer, W., & Lehmann, K. K. 1989, J. Mol. Spectrosc., 134, 134
Smith, A. M., Jørgensen, U. G., & Lehmann, K. K. 1987, J. Chem. Phys., 87, 5649
Snyder, L. E., & Buhl, D. 1971, BAAS, 3, 388
———. 1972, in Ann. NY Acad. Sci., 194, 17
Tennyson, J., Henderson, J. R., & Fulton, N. G. 1995, Comput. Phys. Commun., 86, 175
van Mourik, T., Harris, G. J., Polyansky, O. L., Tennyson, J., Császár, A. G., & Knowles, P. J. 2001, J. Chem. Phys., 115, 3706
Varandas, A. J. C., & Rodrigues, S. P. J. 1997, J. Chem. Phys., 106, 9647